Analytical Cellular Pathology 35 (2012) 129–143
DOI 10.3233/ACP-2011-0047
IOS Press

Review Article: Modern Trends in Imaging V

Optical coherence tomography for rapid tissue screening and directed histological sectioning

Woonggyu Jung[a] and Stephen A. Boppart[b,*]

[a]*Beckman Institute for Advanced Science and Technology, University of Illinois at Urbana-Champaign, Urbana, IL, USA*

[b]*Department of Electrical and Computer Engineering, Bioengineering and Medicine, Beckman Institute for Advanced Science and Technology, University of Illinois at Urbana-Champaign, Urbana, IL, USA*

Abstract. In pathology, histological examination of the tissue is the "gold standard" to diagnose various diseases. It has contributed significantly toward identifying the abnormalities in tissues and cells, but has inherent drawbacks when used for fast and accurate diagnosis. These limitations include the lack of *in vivo* observation in real time and sampling errors due to limited number and area coverage of tissue sections. Its diagnostic yield also varies depending on the ability of the physician and the effectiveness of any image guidance technique that may be used for tissue screening during excisional biopsy. In order to overcome these current limitations of histology-based diagnostics, there are significant needs for either complementary or alternative imaging techniques which perform non-destructive, high resolution, and rapid tissue screening. Optical coherence tomography (OCT) is an emerging imaging modality which allows real-time cross-sectional imaging with high resolutions that approach those of histology. OCT could be a very promising technique which has the potential to be used as an adjunct to histological tissue observation when it is not practical to take specimens for histological processing, when large areas of tissue need investigating, or when rapid microscopic imaging is needed. This review will describe the use of OCT as an image guidance tool for fast tissue screening and directed histological tissue sectioning in pathology.

1. Introduction

Physicians have traditionally relied on their senses, primarily vision and touch, to diagnose illness, monitor a patient's condition, and perform surgical treatments. Over the last few decades, rapid advances in medical imaging technology have greatly enhanced the ability of physicians to diagnose and treat a wide variety of disease [1, 2]. The use of imaging technology has broadened to include imaging before, during, and after surgery, because continuous tissue monitoring can provide accurate diagnosis, clear determination of the surgical area, and confirmation of the surgical margin after a procedure [2–7].

Even though there exists various medical imaging technologies, the most common and historical diagnostic method to identify tissue pathologies is still histological examination. In surgery, the use of many of the existing imaging modalities has been significantly constrained by cost, resolution, and inconvenience of implementation in the surgical suite. Thus, histological examination of tissue is currently the best way to identify pathology at various sites within the body, and it is currently used in a broad range of medical procedures. However, histological analysis is unable to provide an *in vivo*, real time diagnosis because of its inherently

*Corresponding author: Stephen A. Boppart, M.D., Ph.D., Beckman Institute for Advanced Science and Technology, University of Illinois at Urbana-Champaign, Urbana, Illinois, USA. Tel.: +1 217 333-8598; +1 217 244-7479; Fax: +1 217 333-5833; E-mail: boppart@illinois.edu.

time-consuming process and its destructive manner for processing specimens. In addition, only a limited number of biopsies are typically obtained, representing a limited amount of sampling for larger areas of tissue.

Optical coherence tomography (OCT) offers high resolution, minimally invasive, nondestructive, real time imaging [8]. OCT is analogous to ultrasound imaging, but utilizes broadband light instead of sound waves to measure the intensity of back reflection as a function of depth in the tissue. OCT performs micron scale imaging with 1–10 μm resolution and a 2–3 mm depth of imaging which represents the spatial extent of tissue commonly examined in histology. OCT relies on the inherent differences in optical scattering within tissue, and therefore cross-sectional or *en face* images can be generated without the addition of exogenous stains or probes. Remarkably, the morphological features observed by OCT have strong correlation with those observed in histology. Another advantage of OCT is the possible miniaturization of OCT beam delivery systems with optical fiber and micro optics, which can be integrated with endoscopes, microscopes, needle-probes, and handheld scanners. The unique capabilities of OCT offers promise in many medical and surgical applications ranging from fast gross specimen screening and guided histological sectioning to assessing surgical tumor margins during procedures. In particular, OCT can have a powerful impact in the following clinical situations: (1) when excisional biopsy is hazardous or has limited applicability, such as in the eye or the heart; (2) when biopsy sampling needs image guidance for locating small regions of diseased tissue in large areas of interest, such as locating regions of dysplasia in Barrett's esophagus, and thereby reduce sampling errors; (3) when real-time feedback on surgical interventions is required in the operation room, such as assessing tumor margin status during breast lumpectomy procedures; and (4) when pathologists need guidance during gross specimen examination in order to select areas in large tissue specimens for histological sectioning and analysis.

This review will describe the use of OCT as a possible alternative to standard histological processing and as an advanced image-guidance system for practical, efficient, and rapid tissue screening while overcoming limits of current diagnostic methods. This review begins with a technical overview of OCT, including beam delivery devices, and discusses optical biopsy, image-guided diagnostics, and intra-operative image guidance using OCT.

2. Optical coherence tomography

OCT is based on the principle of low coherence interferometry using an optical heterodyne detection scheme to measure small levels of backscattered light from the tissue. An OCT system can be implemented either in free space or by using optical fibers. A schematic of a simple fiber based time domain OCT (TD-OCT) system is shown in Fig. 1 with the main functional components. In the low coherence interferometer, the beam from the light source is launched to one arm of a fiber coupler and split into two paths,

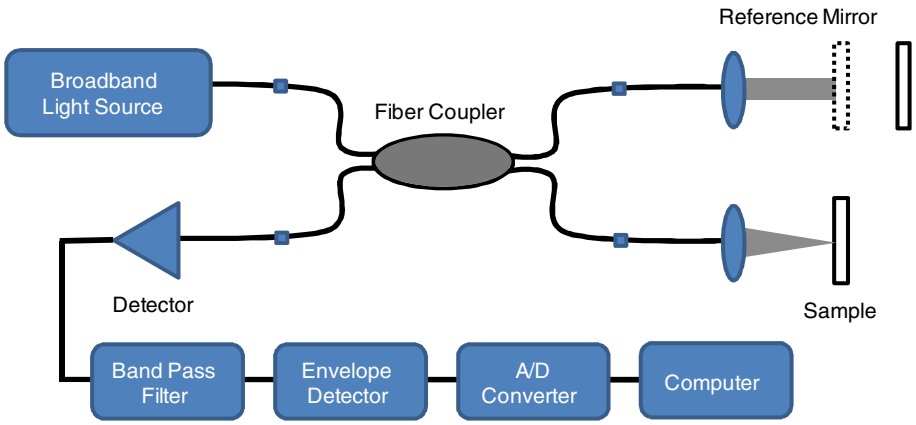

Fig. 1. Schematic representation of a fiber based time domain OCT system. The Michelson interferometer is implemented using a fiber-optic coupler. Light from the low-coherence source is split and sent to a sample arm with a beam delivery instrument and a reference arm with an optical path-length scanner. Reflected light from both arms are combined and is detected with a photodiode in the output of the interferometer.

a reference arm and a sample arm. The beam in the reference arm is reflected off a mirror at a known distance and returns to the detector. The sample beam also reflects from different layers within the tissue, and light returning from the sample and reference arms recombine. If two light beams have traveled the same distance, the two beams will interfere. OCT measures the intensity of interference resulting from different points within the tissue by moving the mirror in the reference arm which generates continuous tissue backscatter information along the depth. As the light in the sample arm is scanned along the lateral direction, the depth-resolved tissue information from each column is appended together and visualized as a 2-D cross-sectional image after signal processing. The axial and lateral resolutions of OCT are determined by the bandwidth of the light source and optics in the sampling arm, respectively. Current OCT technologies have axial resolution ranging from 1 to 15 μm which is more than 10 times higher than standard ultrasound imaging. The intrinsic disadvantage of OCT is the relatively shallow imaging depth around 2–3 mm, depending on tissue type, which is due to the attenuation of the beam as it passes through the tissue [9]. However, this depth is commonly the depth or dimension for histological tissue sections, particularly when examining surgical margins for evidence of tumor cells. OCT can also image internal organs by incorporating OCT beam delivery methods with a wide range of compact imaging probes via optical fiber and micro optics.

Recently, there have been dramatic advances in OCT technology related to imaging speeds. Earlier versions of the OCT system shown in Fig. 1 used a low coherence interferometer with a scanning reference delay arm which detected echo delay signals from tissue in the time domain. It is also possible to perform detection in the Fourier domain by measuring the interferometer spectrum [10]. This method has the advantage of increased sensitivity and signal-to-noise ratio compared to time domain detection because the Fourier domain detection principle measures all the echoes of light simultaneously [11–13]. There are two types of Fourier domain OCT (FD-OCT) systems; one is a spectral domain OCT (SD-OCT) system which uses a spectrometer and line-scan CCD camera [14], and the other is a swept source based OCT (SS-OCT) system which uses a frequency-swept light source having a narrow bandwidth [15]. The greatest advantage of these Fourier domain OCT systems is the increase in imaging speed. Since the data acquisition time of a FD-OCT system is no longer dependent on the mechanical translational speed of the reference arm, it yields significant improvement in imaging speed over the TD-OCT system. For example, most TD-OCT systems acquired less than 500 axial depth scans per second. Current FD-OCT systems can acquire over 100,000 axial depth scans per second, and recent conference reports are demonstrating over 1,000,000 axial depth scans per second. Thus, current high speed OCT systems enable 3-D volumetric imaging which can be used in the clinic [16–18]. In addition, fast signal processing algorithms and high speed platforms such as digital signal processors (DSPs) [19] or graphical processing units (GPUs) [20] can accelerate OCT processing to realize 4-D (3-D plus time) OCT imaging [21].

3. Optical beam delivery of OCT

Compact and portable OCT systems and optical beam delivery instruments are key requirements for performing image-guided histological sampling. The most common OCT system is based on a Michelson interferometer which has four optical paths. Among these, one path is used to deliver optical light to the tissue and collect the back-scattered signal from the tissue. Since OCT systems generate a single axial depth-scan (A-scan) of data through the sample at a time, a stationary focused beam in tissue enables fast axial profile information (1-D data set). In order to obtain a multi-dimensional OCT data set, it is necessary to scan the near-infrared beam laterally across the tissue and assemble adjacent individual axial scans to form 2-D or 3-D images. Numerous optical beam delivery systems for OCT have been introduced, such as research and surgical microscopes [22], hand-held imaging probes [23], catheters and microendoscopes [18, 24], and needles [25, 26] (Fig. 2). Since OCT has a relatively shallow imaging depth, it requires a very compact probe for imaging within the body. Optical beam delivery for OCT can be readily implemented by optical fibers, scanning devices, and micro optics. These can provide access to both external and internal tissue, enable the miniaturization of optical beam delivery, and can be readily integrated within existing medical instruments.

The most common endoscopic OCT probes or catheters are composed of a single-mode optical fiber,

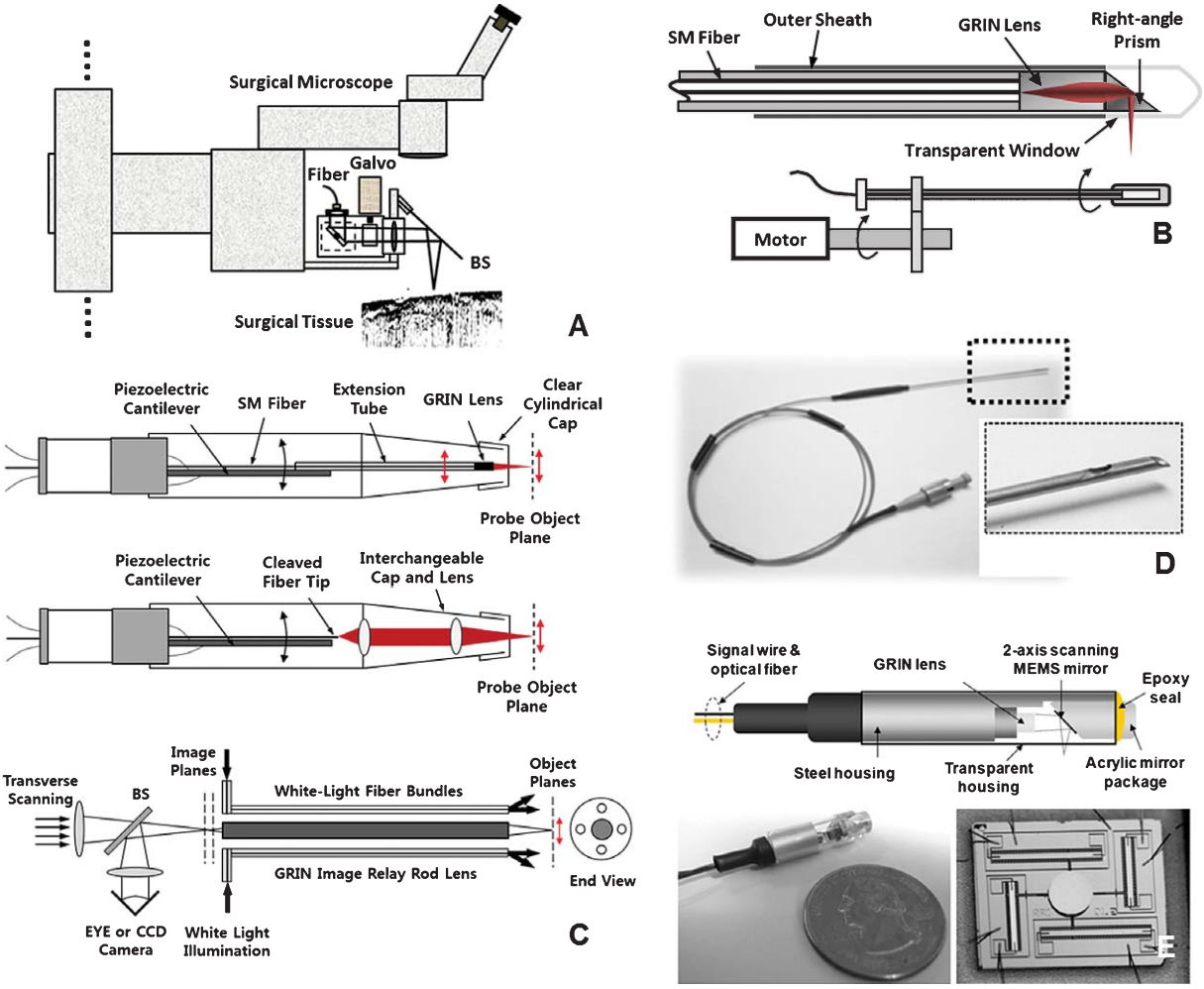

Fig. 2. Beam delivery instruments. Various OCT imaging probe can be implemented which include (A) surgical and research microscope, (B) fiber-optic catheter, (C) hand-held probes and laparoscope, (D) optical needle-probe, (E) 2-D MEMS scanner based endoscopic probe.

GRadient INdex (GRIN) lens, and small prism to deflect focused light onto a tissue. These probes are usually housed in a flexible hollow shaft and are commonly introduced through the working channel of a standard endoscope for simultaneous OCT and video imaging. After finding the tissue location to be imaged using endoscopic visualization, endoscopic OCT probes allow either end-on scanning, linear scanning, or 360° radial scanning for imaging, which depends on the tissue structure and the clinical application. Current *in vivo* endoscopic OCT probes typically have a diameter ranging between 1.0 and 2.5 mm and provide less than 1 mm of working distance from the probe surface. For imaging tubular organs, these probes perform circumferential scanning by rotation [24]. They are also used to image non-tubular or large diameter hollow organs by longitudinal translation [27].

Development of high speed Fourier domain OCT systems have been investigated for high-speed 3-D endoscopic OCT imaging by using conventional probes which rotate continuously during slow longitudinal translation [16, 17]. The use of MEMS (micro-electro-mechanical-systems) scanners for OCT is a rapidly growing area of research due to the fact that the MEMS technology has many advantages over prior designs, including rapid scanning, small size, high reliability, and flexibility in scanning patterns [18]. Efforts for implementing MEMS technology into OCT beam delivery systems have enabled imaging of various internal organs with expanded fields of view.

4. Optical biopsy with OCT

OCT imaging is often referred to as an "optical biopsy" because it enables a real-time image with resolution similar to a standard histological section from a biopsy sample, except without the need for tissue removal [24]. Recent technical advances of OCT in resolution and imaging speed enable the visualization of 3-D microstructure and pathology with extremely high voxel density [28, 29]. There are numerous potential biological tissues for which excisional biopsy is hazardous or impossible to access, but *in vivo*, noninvasive optical biopsy can be used with significant impact.

The most successful application of optical biopsy is ophthalmic imaging. After the invention of OCT in the early 1990's, OCT was first used in ophthalmology for retinal imaging because the eye provides a uniquely suitable medium for OCT due to its transparent nature, minimal scattering, and excellent light penetration [30]. An OCT image can provide detailed cross-sectional structural information of both the anterior and the posterior chamber approaching the resolution of conventional histology [28, 29]. OCT is especially promising for diagnosis and monitoring of a variety of disorders of the papillomacular region of the retina, including glaucoma [31, 32], macula edema [33, 34], macular holes [35], and central serous [36] and age-related macular degeneration [37]. Since OCT images can be analyzed and can provide quantitative information about the corneal and retinal pathology, accurate diagnosis and monitoring of disease progression is possible. A representative example is the detection of glaucoma. The thickness of the retinal nerve fiber layer in a glaucomatous eye in decreased, compared to a normal eye, and OCT can delineate these differences [31] (Fig. 3). The development of fast and smart processing algorithms currently allows the display the 3-D thickness mapping of corneal and retinal layers, which provides statistical data for the screening or management of disease [31, 38]. This advanced technique is also extensively used not only in detection of early disease, but also in many surgical procedures such as LASIK to confirm surgical area [39]. Thus, the use of OCT as an optical biopsy in ophthalmology has the potential to detect and manage a wide spectrum of diseases responsible for loss of vision.

Another potential application of optical biopsy using OCT is to diagnose and characterize coronary artery disease [40, 41]. Coronary artery disease mainly results from atherosclerosis, the deposits of fatty substances, cholesterol, cellular waste products, and other substances in arteries. Assessing atherosclerotic lesions, especially vulnerable plaques that are prone to rupture, has the potential to identify early pathological states that require intervention. Optical biopsy using endoscopic OCT has been shown to be extremely useful for imaging the vascular layers in depth with high micron-scale resolution. Current imaging techniques such as angiography or intravascular ultrasound (IVUS) have difficulty detecting and distinguishing lesions such as vulnerable plaques due to poor resolution [42]. Although OCT cannot visualize deep arterial wall structure like IVUS, its resolution and imaging penetration depth are sufficient to detect unstable plaques. In particular, OCT has high sensitivity and contrast to distinguish lipid rich plaques from other types, because the optical scattering from lipid, adipose and vascular tissue, and calcified plaques are different [40, 41] (Fig. 4). OCT also has an advantage in terms of size of catheter, compared to an IVUS catheter. An OCT catheter uses a single mode optical fiber (125 μm in diameter) and micro optics rather

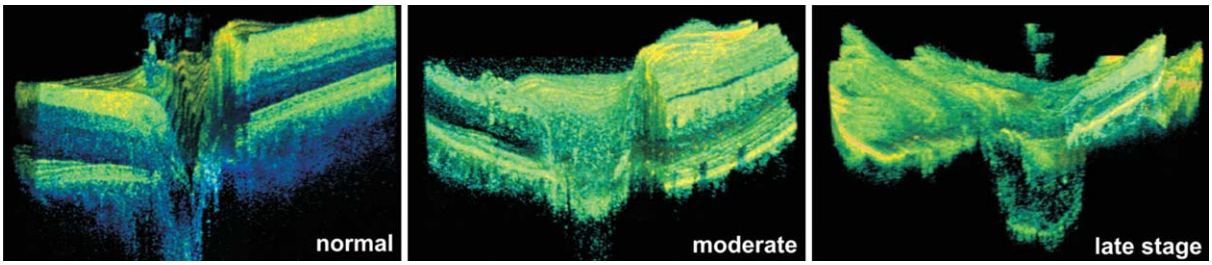

Fig. 3. 3-D visualization of the human retinal nerve fiber layer from a normal optic nerve head (left), intermediate stage glaucoma (middle), and advanced glaucoma (right). The different elevation of the papilla are clearly visible. Figure reprinted with permission from [31].

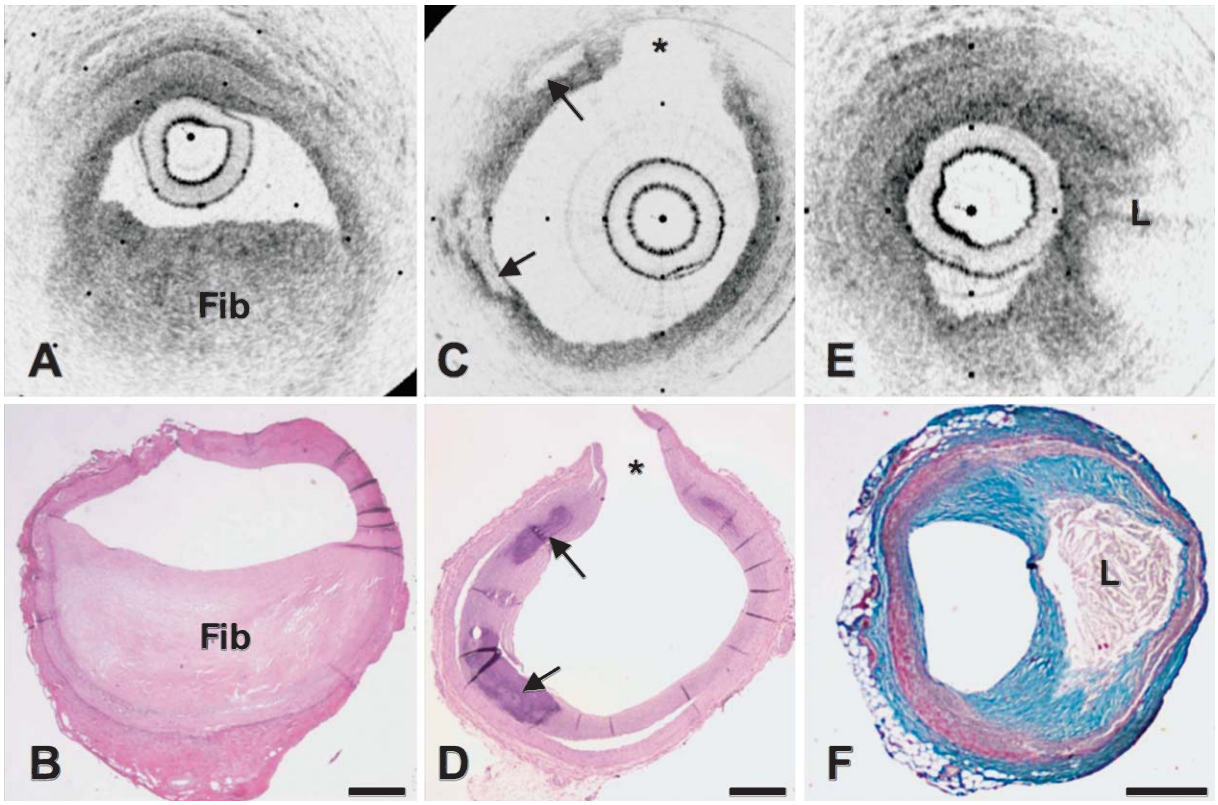

Fig. 4. OCT images and corresponding histology for (A, B) fibrous, (C, D) calcific, and (E, F) lipid-rich plaque types. Abbreviations: Fib, fibrous plaques; L, lipid-rich regions. Arrows indicate calcific regions. Asterisks show correlating features. Scale bars represent 500 μm. Figure used with permission from [40].

than a piezoelectric transducer, and therefore can be constructed as inexpensive, flexible, and thin wire-like probes. Thus, catheter-based intravascular OCT has the potential for imaging regions of tight stenosis or small vessels located more distally in the vascular system, all of which could lead to significant improvements in diagnostic capabilities.

Optical biopsy of the vocal cords is also of particular importance given the delicate nature of the vocal cord mucosa [43]. This is because excisional biopsy can damage the mechanical characteristics of the cords and lead to alteration of the mucosal wave during phonation, leading to a change in voice. In current practice, to ensure adequate resection of malignant lesions, a wider margin is usually taken, which leads to greater than necessary risks for voice changes. In addition to these examples, there are many other potential tissue sites in which an optical biopsy with OCT can be used with significant clinical impact such as muscle [44], cartilage [45], and nerve [46].

5. Image-guided biopsy using OCT

Many endoscopic procedures of internal organs could benefit from improvements in image-guided biopsy, rather than performing random biopsies, or biopsies guided by video-based imaging of the tissue surface. Image guidance offers the advantage of screening large areas of tissue and aids in identifying potentially diseased locations from where biopsies will be taken. Various imaging techniques have been developed for this purpose, but the most common image guidance tool currently used is conventional video endoscopy. Imaging modalities such as x-ray computed tomography (CT), magnetic resonance imaging (MRI), and positron emission tomography (PET) have been mostly used outside the procedure or operating room. Even though there have been efforts to transform these cross-sectional imaging modalities into procedural or surgical guidance tools, these techniques have their limitations, such as resolution, size, cost, or use

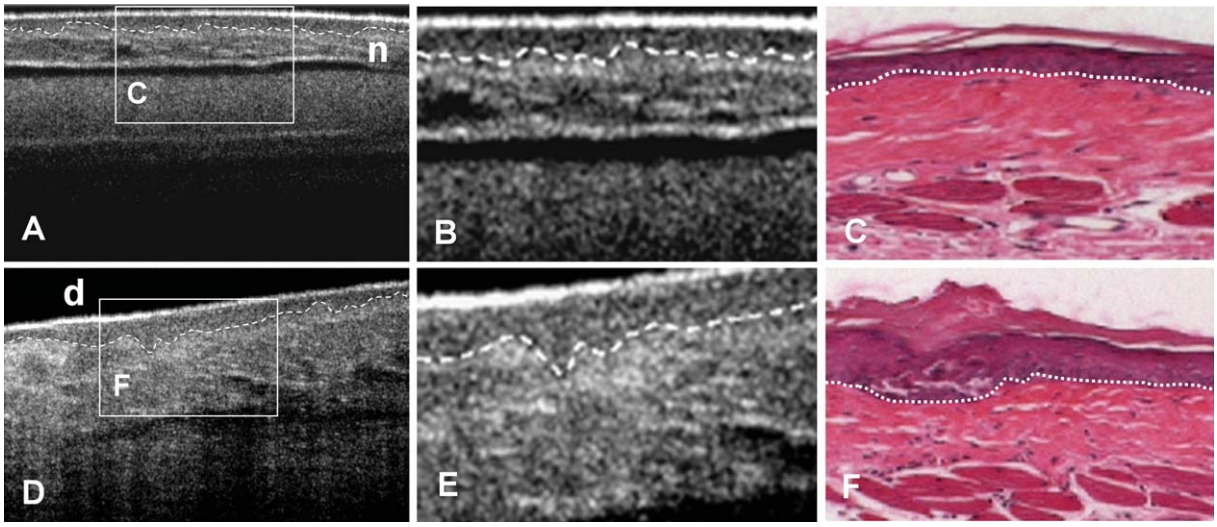

Fig. 5. *In vivo* OCT images of hamster cheek pouch with dysplasia. (A–C) OCT image of normal hamster cheek pouch and corresponding histology; (D–F) OCT image of hamster cheek pouch with dysplasia and corresponding histology; The OCT images are 2×1.3 mm with 10×10 μm display resolution. (B) and (E), higher magnification views of (A) and (D), respectively. The location of the basement membrane is indicated by the dotted lines. Abbreviations: n, normal epithelial and subepithelial layer; d, area of dysplasia with epithelial down growth. Figure used with permission from [55].

in imaging regions that are difficult to access [47–50]. Endoscopic ultrasound (US) imaging has become a routine procedure for detecting a variety of diseases, including cancer of internal organs [51–54], but there still remains some critical limitations in the use of US for distinguishing benign processes from early-stage malignancy or assessment of treatment results due to its low spatial resolution and necessity of acoustic coupling between the transducer and tissues.

Optical endoscopes are portable, indispensible tools in many procedures, and offer a magnified view. However, they are somewhat limited in their ability as an image guidance tool for comprehensive tissue screening because conventional bright-field endoscopes do not provide detailed information on tissue structure below the surface. This limitation can often result in a sampling error when abnormal tissue is present below a normal mucosa or tissue surface. The use of OCT as an endoscopic image guidance tool can be a solution for overcoming many of the drawbacks in the current methods. In particular, its capability to detect microscopic sub-surface tissue abnormalities, most often representing early-stage disease, is the most important merit for screening large areas of tissue.

A major OCT application is the detection of cancerous and precancerous states in epithelial tissue, which frequently arise within ~500 μm beneath the surface, a depth well-suited for OCT. OCT typically images tissue morphology with contrast derived from tissue scattering. The disruption of tissue architecture from carcinomas dramatically changes the optical scattering properties, and OCT can detect these changes with high sensitivity. The variation of refractive index of tissue can also be used to differentiate between normal and cancerous tissues. With these light–tissue interactions, OCT has been used to detect early-stage cancer in a broad-range of internal organs such as the digestive, respiratory, urinary, and genital tracts, and the oral cavity. Figure 5 shows an example of OCT imaging of precancerous dysplasia. In an oral cancer study using a hamster cheek pouch model, OCT was able to differentiate between normal cheek tissue, cheek tissue with dysplasia, and cheek tissue with squamous cell carcinoma [55], and had good agreement with corresponding histological examinations.

There are many other diseases for which a number of morphological changes can be observed in the superficial layers of tissue during disease progression, such as an increase in epithelial thickness and alterations in extracellular matrix architecture. OCT has been extensively used to visualize these structural changes in superficial layers of tissues [56, 57]. The monitoring of inhalation injury using OCT is one such example. In studies related to inhalation pathology, OCT was

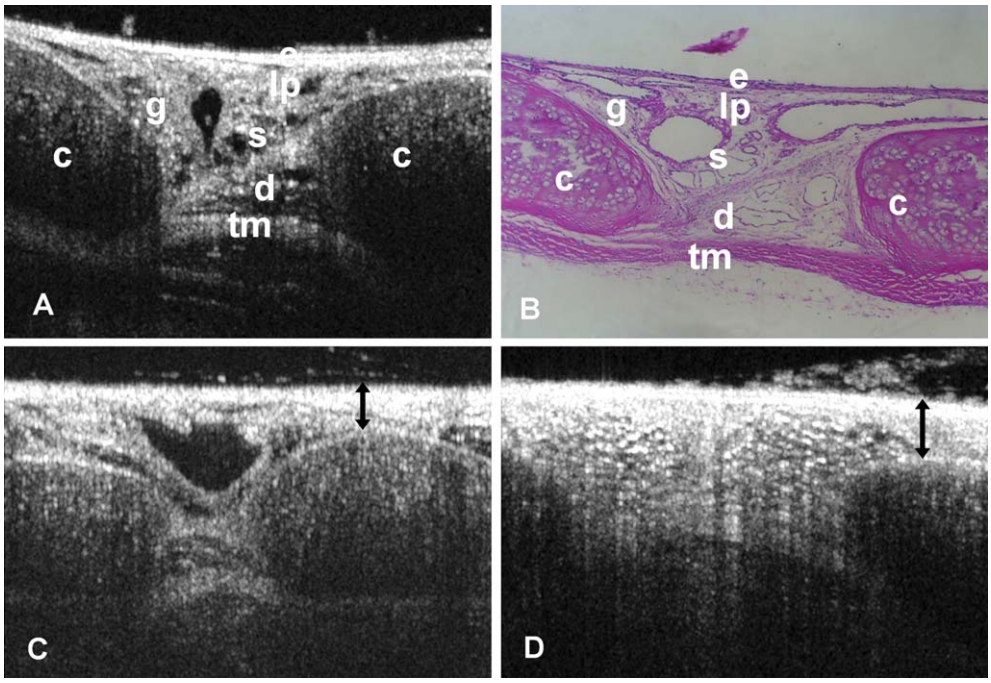

Fig. 6. Respiratory tract imaging. Comparison between (A) OCT and (B) corresponding H&E section. Comparison of OCT images obtained from (C) normal and (D) septic rabbit trachea. In contrast to normal trachea, mucosal and submucosal edema is observed in the septic trachea. Arrows indicate difference in tissue thickness/swelling between normal and septic rabbit tracheas. The OCT images are 2×1.3 mm with 10×10 μm pixel size. Abbreviations: c, cartilage; e, epithelium; g, glands; lp, lamina propria; d, dense fibro elastic-tissue; s, submucosa; tm, tunica muscularis. Figure used with permission from [56].

capable of detecting swelling, edema, and obstruction of the airway, showing clear tissue morphology including epithelium, mucosa, cartilage, and glands in tracheal tissues [56] (Fig. 6). All of these studies, and many others, have demonstrated that OCT images correlate extremely well with corresponding histological sections. OCT can also provide images of the 3-D morphological structure over large areas, and in real-time, which cannot be achieved with other imaging modalities and biopsy. Thus, the unique capabilities of OCT promise to rapidly identify suspect regions and to guide excisional biopsy while reducing the likelihood of false negatives due to sampling errors.

6. Intraoperative image guidance using OCT

A surgical microscope is routinely used to guide delicate surgery by magnifying the surface features of tissue. The development of advanced imaging techniques capable of high resolution and real time visualization of sub-surface tissue structure could provide additional useful information to guide the intervention. For example, this advanced imaging modality could be used intraoperatively to localize a tumor, to help define the tumor margin, and to determine the margin status (positive or negative of tumor cells) and if any residual tumor remains. OCT is very suitable for this application, and can be adapted to the surgical environment to fulfill these current needs. OCT inherently satisfies many of the design requirements for an intraoperative imaging guidance tool, and can also readily be integrated into an existing surgical microscope or implemented as hand-held surgical imaging probes. Thus, the imaging capabilities of OCT permit the intra-operative guidance and monitoring of the surgical procedure, giving immediate image-based feedback to the surgeon. There are two types of situations where OCT can potentially be used as an intraoperative imaging tool: (1) *ex vivo* imaging to assess the surgical margin on resected tissue, and (2) *in vivo* or *in situ* imaging of tissue before, during, and after surgical resection. Even though OCT image guidance can be applied to many types of surgical oncology procedures, here we introduce as a

representative example the use of intraoperative OCT in breast cancer surgery, which has been an emerging surgical application of OCT. Intraoperative OCT can also be used in other solid tumor surgeries including those for brain, lung, liver, kidney, thyroid, pancreatic, and colon cancers, among many others.

In the past, a standard surgical procedure to treat breast cancers was radical mastectomy. Currently, a breast conserving lumpectomy procedure is often the preferred surgical treatment, with the goal to leave the natural appearance and cosmetic quality of the breast mostly intact while removing the cancerous tissue. After the lumpectomy, the resected tumor mass and tissue are sent to a pathologist, where the margin status is determined using most commonly H&E stained histology and light microscopy. Depending on the institution and how much breast tissue is conserved, relative to the tumor tissue, positive margin and re-operation rates can be as high as 40% [58]. This process of post-operative microscopic assessment of limited regions of the surgical margin is inefficient in terms of tissue sampling, time, and cost. High resolution OCT may be an alternative solution for rapid and accurate intraoperative assessment of breast cancer margins. OCT can immediately image resected breast tissue and provide fast feedback to the surgeon inside the operating room. OCT images have differentiated cancerous, fibrous, and fatty tissue due to different optical scattering properties of each tissue type [22]. In addition, the high resolution of OCT permits identification of small (<1 mm) foci of tumor cells, which are not visible by visual inspection alone. Many studies have shown good correlation between structural information acquired with OCT and the corresponding histology. One of the most recent studies demonstrated the potential of real time intra-operative OCT for margin assessment from 37 resected breast lumpectomy specimens [59]. In this study comprised of a training set and a study set of patients, OCT classified surgical margins as positive or negative, compared to histologic findings, and achieved 100% sensitivity and 82% specificity. Figure 7 shows representative OCT images

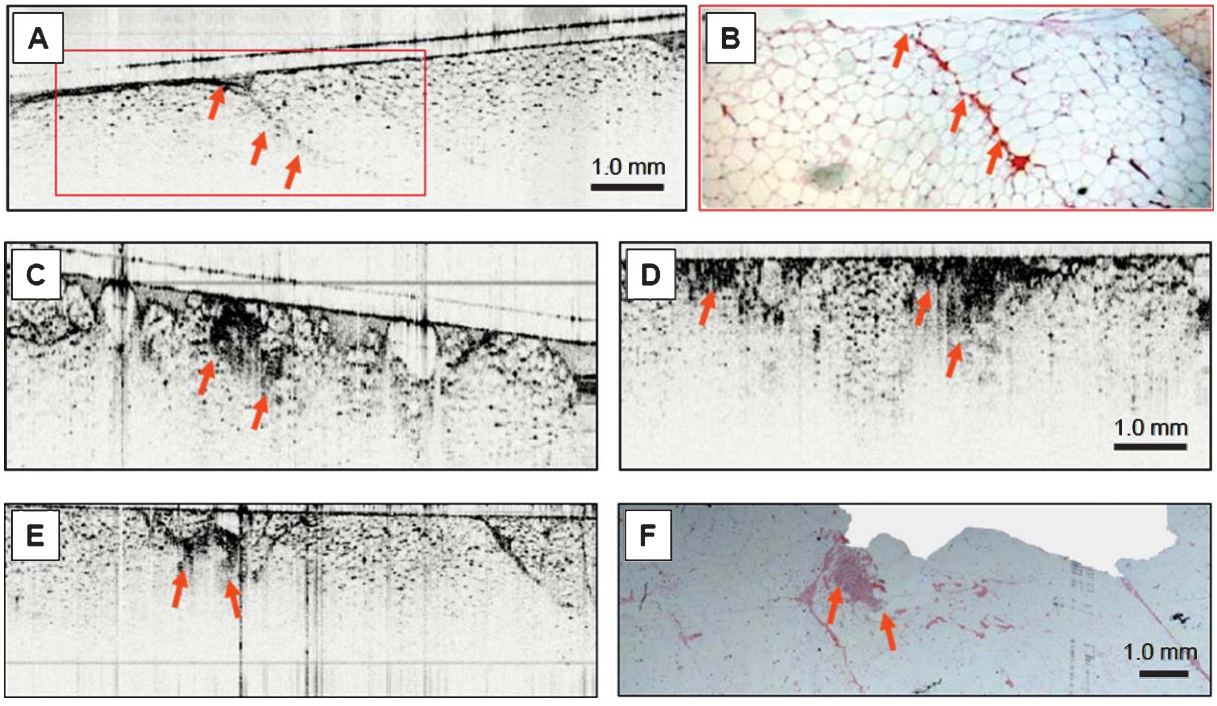

Fig. 7. Intra-operative surgical margin assessment with OCT, and corresponding histology, from a breast cancer lumpectomy procedure. (A) OCT image of a negative surgical margin composed primarily of adipose tissue. The small dark highly scattering point-like features correspond to individual nuclei of adipocytes, and arrows indicate vasculature. (B) Corresponding histology. (C) OCT image of a positive margin with ductal carcinoma *in situ* (arrows indicate dense highly-scattering features corresponding to tumor cells). (D) OCT image of a positive margin with invasive ductal carcinoma (tumor cell features indicated by arrows). (E) OCT image and (F) corresponding histology of a small isolated focus of tumor cells at the surgical margin. Figure used with permission from [59].

and corresponding histological observations from this study. These findings suggest that OCT is a potential method for the real-time intraoperative assessment of margin status in lumpectomy procedures.

Lumpectomy procedures may often include the removal of regional lymph nodes, which typically includes a sentinel lymph-node dissection. This procedure may be accompanied by the removal of additional axillary lymph nodes to help stage disease progression. Although a number of lymph nodes are often resected during sentinel lymph-node dissections, only a relatively small percentage of nodes are found to be metastatic. Thus, there is significant need for an intraoperative nodal assessment imaging technology to reduce the percentage of normal nodes that are resected during lymph node dissection procedures, or to provide the yes/no determination of metastatic involvement for each lymph node. To demonstrate feasibility, OCT was initially used to image lymph nodes microarchitecture from a carcinogen-induced rat mammary tumor model [60]. In this study, three-dimensional OCT imaging of lymph nodes enabled visualization of anatomical features such as the capsule, lymphoid follicles, cortex, and medullary sinuses and showed good correlation with histology. OCT was also used intraoperatively to compare image-based features of normal, reactive, and metastatic axillary lymph nodes [61] (Figs. 8, 9). OCT images from normal lymph nodes showed that a highly scattering capsule structure can be readily distinguished from the lower scattering cortex of the lymph nodes. In contrast, the distinct boundary between the capsule and the cortex was no longer visible in reactive and metastatic nodes where the entire node becomes more highly scattering, matching the scattering intensity level from the capsule, and forming a single homogeneous scattering layer. In all cases, OCT images showed good correlations with corresponding histology.

Currently, x-ray imaging or histological analysis of resected masses can provide feedback to the surgeon during breast surgery. However, there is no real time, nondestructive intraoperative method to assess the lumpectomy margins in breast cancer tissues or the status of lymph nodes. OCT is a potential candidate for *in situ* or *in vivo* imaging in the operating room and can be used to image and identify tumor margins before resecting tissue. Since the surgeon can remove the cancerous tissue while monitoring the margin status using OCT, there is the potential to significantly reduce the amount of normal tissue resected. The surgeon can also directly reconfirm the tumor margin from the resected mass in a short period of time with the OCT images.

The same procedure can also be applied to lymph node dissection. Intraoperative OCT can minimize the

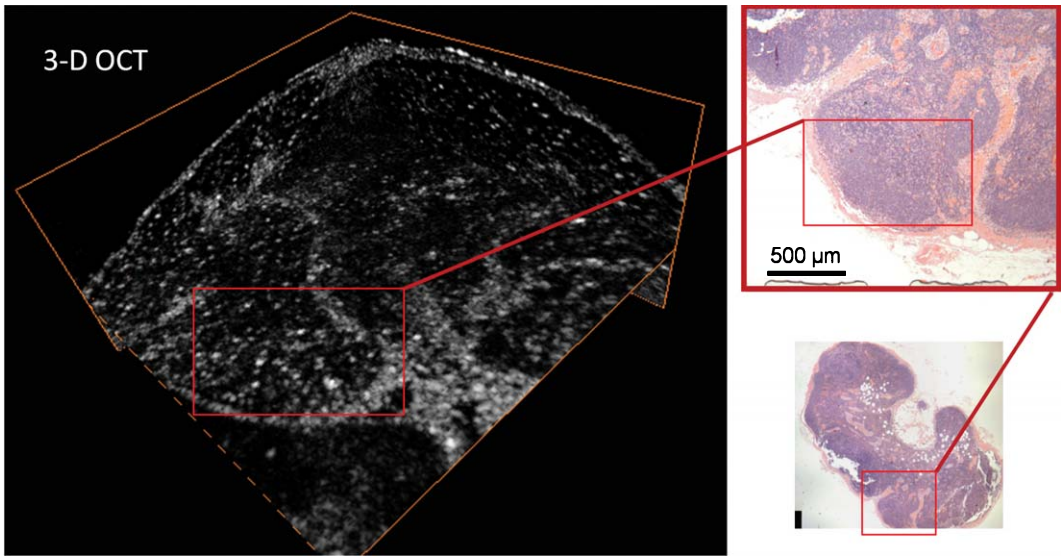

Fig. 8. 3-D OCT image and corresponding histology of a normal sentinel lymph node. The normal lymph node shows a clear capsule that is easily differentiated from the low-scattering cortex. The OCT image correlates to the regions in the histology that are highlighted by the red boxes. The volume of the 3-D OCT dataset is $5\times5\times1.7\,\text{mm}^3$. Figure used with permission from [61].

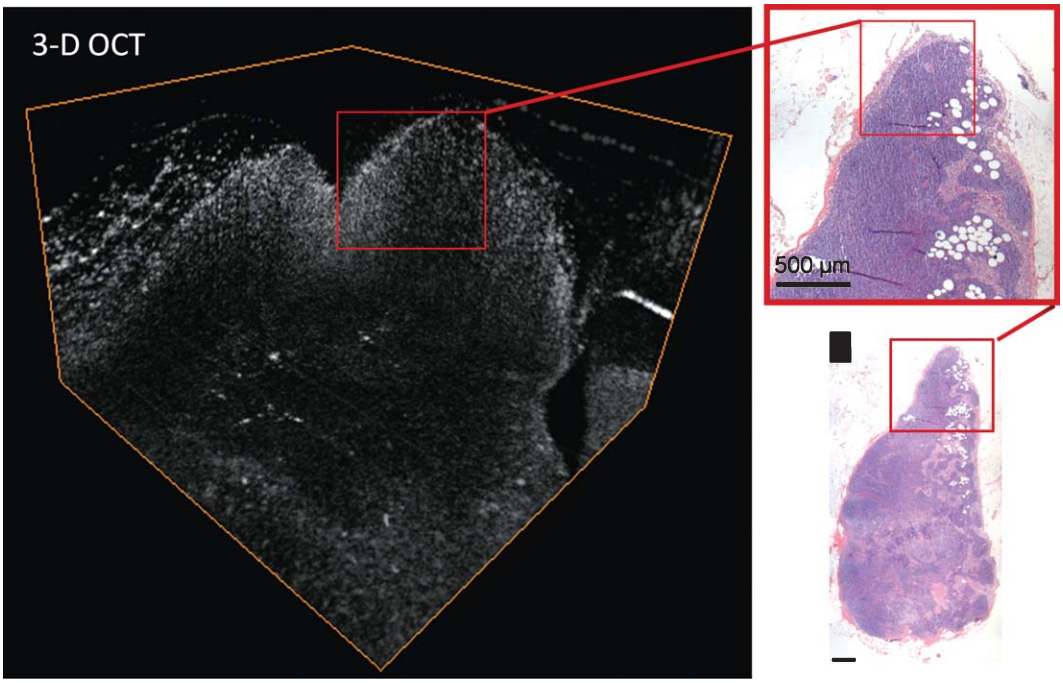

Fig. 9. 3-D OCT image and corresponding histology of a metastatic axillary lymph node. As with reactive lymph nodes, increased scattering from the node is observed in the OCT data, and the ability to differentiate distinct boundaries between the node capsule and cortex has been lost. The OCT image correlates to the regions in the histology that are highlighted by the red boxes. The volume of the 3-D OCT dataset is $5 \times 5 \times 1.7\,\text{mm}^3$. Figure used with permission from [61].

risk of morbid complications such as lymphedema, which is associated with the lymph node dissections for breast cancer staging. To accomplish this, the primary requirement is the implementation of a compact hand held probe for *in situ* and *in vivo* patient imaging. However, the realization of an *in situ* or *in vivo* intraoperative OCT system has numerous challenges. One of the main challenges is the need for fast, real time OCT imaging at micron-scale resolutions over large fields of view often tens to hundreds of square centimeters in area. In many circumstances, a surgeon might prefer to use a simpler manually-scanned handheld probe to obtain OCT images of tissues and organs which might otherwise be inaccessible using standard mechanical-scanning probes. Recently a manual scanning technique has been reported for OCT that can image over a large field of view with user defined scanning geometry [62]. In this study, a novel cross correlation based image acquisition technique for OCT was introduced that enables sensor-less manual lateral scanning. Manually-scanned OCT images have good correlation with OCT images acquired by mechanical scanning. This method can not only provide an extension of the field of view of current OCT imaging, but can also be integrated with needle-based OCT for deep tissue imaging. Another challenge is the rapid interpretation of the large amounts of data generated by imaging large 3-D volumes of tissue during surgery. Image analysis techniques may be used for guidance and detection of tumors [63]. A multi-sensory representation of OCT data may be another way to facilitate rapid interpretation in time sensitive surgical or diagnostic procedures [64]. This approach uses sound to represent OCT data and can complement visual data without requiring the surgeon to constantly monitor the display screen. Additionally, sound representation of optical scattering data may be used in non-imaging procedures such as optically-guided needle biopsies.

7. Conclusions

In the past, identifying and diagnosing tissue pathology has most often been performed with stained histological sections observed by white-light

microscopy in the pathology department. The high resolution, real time imaging capabilities of OCT may enable these histopathological observations and diagnoses to be made intraoperatively. OCT may also find application in guiding the selection of biopsy sites when large areas of tissue are investigated, and biopsy sampling is limited. In cases where tissue biopsy confers high risks, such as in the eye, heart, or brain, OCT images may be used to directly make diagnostic decisions. Finally, in the pathology lab, where large gross specimens are visually examined to determine where microscopic sections are to be taken, real-time OCT may be used to rapidly image large areas of tissue in search for microscopic evidence of disease, and guide the pathologist to select suspicious sites for histopathological examination. Undoubtedly, the imaging capability of OCT has the potential to offer a more efficient diagnostic assessment in terms of cost and time, and may offer a new paradigm for tissue imaging, assessment, and monitoring in the operating room. Currently, there are many ongoing OCT studies ranging from technology development to large scale clinical studies that will help validate the use of OCT and move it more toward the standard of care.

In the last few years, the development of FD-OCT systems has accelerated the clinical impact of OCT for monitoring disease with its real-time imaging capability. However, further technological improvements are still needed to develop and fully demonstrate the advantages of 3D OCT imaging because the speed of current FD-OCT systems are still not sufficient for real-time 3D visualization. In many cases, high speed OCT first acquires 3D data sets, and then uses off-line post-processing of the data to visualize 2D and 3D images. Complete visualization of continuous 2D and 3D images, while saving image data, requires extensive computation, imaging processing, and memory assignment by the CPU (central processing unit), making the system slower and more sensitive to motion artifacts. Utilizing the computational capabilities of GPU's (graphical processing units) can significantly overcome these limitations [20, 65], and potentially realize even 4D (3D volumes over time) imaging.

Ongoing research is also investigating means to enhance image contrast in OCT [66, 67]. Even though current OCT techniques can offer high (micron) resolution imaging, this frequently remains insufficient to accurately characterize tissue and to differentiate important pathology such as cancer at the cellular or molecular level. In order to overcome this challenge, various engineered contrast agents specifically designed for OCT have been developed and characterized. In particular, magnetomotive OCT using magnetic nanoparticles is one very promising technique for selective molecular imaging of tumors [68]. Nanoparticles can be functionalized with antibodies or ligands to target them to specific molecules, cells, or tissue types [69]. These dynamic contrast agents change the local scattering properties of the tissue microenvironment during OCT imaging when a small external magnetic field is applied and modulated. Thus, the use of novel contrast agents will provide additional selectivity for OCT, and can also be used to measure mechanical properties of tissues and potentially even cells in a variant called optical coherence elastography [70]. Finally, gold and iron-oxide nanoparticles may be used as therapeutic agents because their strong optical absorption and magnetic heating properties, respectively, can induce local hyperthermia in cells and tissues.

Functional extensions of OCT can provide valuable information about tissues which is not present in structural OCT images. Functional OCT include optical Doppler tomography (ODT) [71], polarization-sensitive OCT (PS-OCT) [72], spectroscopic OCT [73], second harmonic OCT [74], and nonlinear interferometric vibrational imaging (NIVI) [75, 76], a technique that uses optical interferometry to measure coherent anti-Stokes Raman scattering (CARS) signals based on molecular vibrations. Structural OCT utilizes only the amplitude of back-scattered light from the tissue for image formation, whereas ODT additionally employs interferometric phase information to monitor Doppler frequency shifts in the back-scattered spectrum. Thus, ODT is capable of producing simultaneous imaging of both the tissue architecture and profiles of blood flow. ODT has been used to a number of applications, mainly blood-flow mapping in subsurface vessels in skin and retina. The most active application is to use ODT for the diagnosis of a number of retinal diseases including glaucoma and diabetic retinopathy. PS-OCT is another functional variation of OCT which exploits the birefringence properties in highly ordered tissue. Many biological components (collagen, elastin, muscle fibers, nerve fibers) in tissues such as eye, skin, teeth, and muscle contain intrinsic birefringence or form birefringence. PS-OCT measures the change of polarization state compared to the incident state of polarized light along the depth of the interrogation region. This measurement provides an additional con-

trast mechanism for OCT in terms of polarization that is not discernible using standard optical diagnostic methods. Moreover, PS–OCT is an attractive technique in laser surgical procedures to monitor the tissue response during laser treatment since most laser surgery is based on photo-thermal mechanisms which produce birefringence changes in subsurface tissue components.

The information provided by advanced OCT techniques in terms of speed, resolution, and contrast could further improve our ability to diagnosis disease at earlier stages, further improve the identification of tumor margins intraoperatively, and further improve the rapid identification and assessment of pathological changes, both inside and outside the pathology laboratory. The OCT technology is highly modular and flexible, and can be applied to many medical and surgical specialties, in addition to oncology. This flexibility also provides the potential to contribute at multiple stages of clinical care such as screening, biopsy guidance and diagnosis, endoscopic or open surgical guidance, and monitoring of treatments. OCT is not likely to replace biopsy and histopathology, the gold standard for diagnosis. However, as described here, there are multiple applications where OCT can play a highly complementary role in offering the real-time microscopic assessment and imaging of tissues in the endoscopy suite, the operating and procedures rooms, and in the pathology laboratory.

References

[1] J.V. Frangioni, "New technologies for human cancer imaging", *Journal of Clinical Oncology* **26** (2008), 4012–4021.

[2] T. Peters and K. Cleary, *Image-guided interventions: Technology and applications* springer, 2007.

[3] J.T. Yap et al., "Image-guided cancer therapy using PET/CT", *Cancer Journal* **10** (2004), 221–233.

[4] T. Tjardes et al., "Image-guided spine surgery: State of the art and future directions", *European Spine Journal* **19** (2010), 5–45.

[5] A.H. Chan et al., "*In vivo* feasibility of image-guided transvaginal focused ultrasound therapy for the treatment of intracavtary Fibroids", *Fertility and Sterility* **82** (2004), 723–730.

[6] D.W. Roberts et al., "Intra-operative image updating", *Stereotactic and Functional Neurosurgery* **76** (2001), 148–150.

[7] R.S. Hinks et al., "MR systems for image-guided therapy", *Journal of Magnetic Resonance Imaging* **8** (1998), 19–25.

[8] D. Huang et al., "Optical Coherence Tomography", *Science* **254** (1991), 1178–1181.

[9] J.M. Schmitt, "Optical coherence tomography (OCT): A review", *IEEE Journal of Selected Topics in Quantum Electronics* **5** (1999), 1205–1215.

[10] A.F. Fercher et al., "Measurement of intraocular distances by backscattering spectral interferometry", *Optics Communications* **117** (1995), 43–48.

[11] R. Leitgeb et al., "Performance of Fourier domain vs. time domain optical coherence tomography", *Optics Express* **11** (2003), 889–894.

[12] J.F. de Boer et al., "Improved signal-to-noise ratio in spectral-domain compared with time-domain optical coherence tomography", *Optics Letters* **28** (2003), 2067–2069.

[13] B. Liu and M.E. Brezinski, "Theoretical and practical considerations on detection performance of time domain, Fourier domain, and swept source optical coherence tomography", *Journal of Biomedical Optics* **12**(1-12), (2007), 044007.

[14] S.H. Yun et al., "High-speed spectral-domain optical coherence tomography at 1.3 μm wavelength", *Optics Express* **11** (2003), 3598–3604.

[15] S.H. Yun et al., "High-speed optical frequency-domain imaging", *Optics Express* **11** (2003), 2953–2963.

[16] S.H. Yun et al., "Comprehensive volumetric optical microscopy *in vivo*", *Nature Medicine* **12** (2006), 1429–1433.

[17] D.C. Adler et al., "Three-dimensional endomicroscopy using optical coherence tomography", *Nature Photonics* **1** (2007), 709–716.

[18] W. Jung et al., "*In vivo* three-dimensional spectral domain endoscopic optical coherence tomography using a microelectromechanical system mirror", *Optics Letters* **32** (2007), 3239–3241.

[19] J.P. Su et al., "Real-time swept source optical coherence tomography imaging of the human airway using a microelectromechanical system endoscope and digital signal processor", *Journal of Biomedical Optics* **13** (1-3), (2008), 030506.

[20] Y. Watanabe and T. Itagaki, "Real-time display on Fourier domain optical coherence tomography system using a graphics processing unit", *Journal of Biomedical Optics* **14** (1-3), (2009), 060506.

[21] M.W. Jenkins et al., "4D embryonic cardiography using gated optical coherence tomography", *Optics Express* **14** (2006), 736–748.

[22] S.A. Boppart et al., "Optical coherence tomography: Feasibility for basic research and image-guided surgery of breast cancer", *Breast Cancer Research and Treatment* **84** (2004), 85–97.

[23] S.A. Boppart et al., "Forward-imaging instruments for optical coherence tomography", *Optics Letters* **22** (1997), 1618–1620.

[24] G.J. Tearney et al., "*In vivo* endoscopic optical biopsy with optical coherence tomography", *Science* **276** (1997), 2037–2039.

[25] X. Li et al., "Imaging needle for optical coherence tomography", *Optics Letters* **25** (2000), 1520–1522.

[26] A.M. Zysk et al., "Needle-based reflection refractometry of scattering samples using coherence-gated detection", *Optics Express* **15** (2007), 4787–4794.

[27] B.E. Bouma and G.J. Tearney, "Power-efficient nonreciprocal interferometer and linear-scanning fiber-optic catheter for optical coherence tomography", *Optics Letters* **24** (1999), 531–533.

[28] B. Povazay et al., "Impact of enhanced resolution, speed and penetration on three-dimensional retinal optical coherence tomography", *Optics Express* **17** (2009), 4134–4150.

[29] I. Grulkowski et al., "Anterior segment imaging with spectral OCT system using a high-speed CMOS camera", *Optics Express* **17** (2009), 4842–4858.
[30] M.R. Hee et al., "Optical coherence tomography of the human retina", *Archives of Ophthalmology* **113** (1995), 325–332.
[31] B. Povazay et al., "Minimum distance mapping using three-dimensional optical coherence tomography for glaucoma diagnosis", *Journal of Biomedical Optics* **12** (1-8), (2007), 041204.
[32] G. Vizzeri et al., "Spectral domain-optical coherence tomography to detect localized retinal nerve fiber layer defects in glaucomatous eyes", *Optics Express* **17** (2009), 4004–4018.
[33] R.J. Campbell et al., "Optimal optical coherence tomography-based measures in the diagnosis of clinically significant macular edema: Retinal volume vs. foveal thickness", *Arch Ophthalmolology* **125** (2007), 619–623.
[34] S. Wolf, "Assessing diabetic macular edema with optical coherence tomography", *Medical Retina* Springer Berlin Heidelberg, (2010), 125–129.
[35] M. Hangai et al., "Three-dimensional imaging of macular holes with high-speed optical coherence tomography", *Ophthalmology* **114** (2007), 763–773.
[36] Y. Ojima et al., "Three-dimensional imaging of the foveal photoreceptor layer in central serous chorioretinopathy using high-speed optical coherence tomography", *Ophthalmology* **114** (2007), 2197–2207.
[37] Y. Chen et al., "Three-dimensional ultrahigh resolution optical coherence tomography imaging of age-related macular degeneration", *Optics Express* **17** (2009), 4046–4060.
[38] M. Wojtkowski et al., "Comparison of reflectivity maps and outer retinal topography in retinal disease by 3-D Fourier domain optical coherence tomography", *Optics Express* **17** (2009), 4189–4207.
[39] M. Avila et al., "High-speed optical coherence tomography for management after laser *in situ* keratomileusis", *Journal of Cataract and Refractive Surgery* **32** (2006), 1836–1842.
[40] G.J. Tearney et al., "Optical coherence tomography for imaging the vulnerable plaque", *Journal of Biomedical Optics* **11**, 021002 (1-10), 2006.
[41] I.K. Jang et al., "*In vivo* characterization of coronary atherosclerotic plaque by use of optical coherence tomography," *Circulation* **111** (2005), 1551–1555.
[42] T. Kume et al., "Assessment of coronary arterial plaque by optical coherence tomography", *American Journal of Cardiology* **97** (2006), 1172–1175.
[43] B. Wong, "*In vivo* optical coherence tomography of the human larynx: Normative and benign pathology in 82 patients," *Laryngoscope* **116** (2006), 507–507.
[44] B.R. Klyen et al., "Three-dimensional optical coherence tomography of whole-muscle autografts as a precursor to morphological assessment of muscular dystrophy in mice", *Journal of Biomedical Optics* **13** (1-7), (2008), 011003.
[45] C.R. Chu et al., "Clinical optical coherence tomography of early articular cartilage degeneration in patients with degenerative meniscal tears", *Arthritis and Rheumatism* **62** (2010), 1412–1420.
[46] S.A. Boppart et al., "Intraoperative assessment of microsurgery with three-dimensional optical coherence tomography", *Radiology* **208** (1998), 81–86.
[47] S.V. Ghate et al., "MRI-guided vacuum-assisted breast biopsy with a handheld portable biopsy system", *American Journal of Roentgenology* **186** (2006), 1733–1736.
[48] E.R. McVeigh et al., "Real-time interactive MRI-guided cardiac surgery: Aortic valve replacement using a direct apical approach", *Magnetic Resonance in Medicine* **56** (2006), 958–964.
[49] M.A. Rafferty et al., "Investigation of C-arm cone-beam CT-guided surgery of the frontal recess", *Laryngoscope* **115** (2005), 2138–2143.
[50] S.A. Gulec, "PET probe-guided surgery", *Journal of Surgical Oncology* **96** (2007), 353–357.
[51] J.E. Hartley et al., "Laparoscopic ultrasound for the detection of hepatic metastases during laparoscopic colorectal cancer surgery", *Diseases of the Colon &Rectum* **43** (2000), 320–324.
[52] S. Kelly et al., "A systematic review of the staging performance of endoscopic ultrasound in gastro-oesophageal carcinoma", *Gut* **49** (2001), 534–539.
[53] S.S. Kaplan, "Clinical utility of bilateral whole-breast US in the evaluation of women with dense breast tissue", *Radiology* **221** (2001), 641–649.
[54] D.B. Williams et al., "Endoscopic ultrasound guided fine needle aspiration biopsy: A large single centre experience", *Gut* **44** (1999), 720–726.
[55] W. Jung et al., "Advances in oral cancer detection using optical coherence tomography", *IEEE Journal of Selected Topics in Quantum Electronics* **11** (2005), 811–817.
[56] W. Jung et al., "Feasibility study of normal and septic tracheal imaging using optical coherence tomography", *Lasers in Surgery and Medicine* **35** (2004), 121–127.
[57] E.V. Zagaynova et al., "*In vivo* optical coherence tomography feasibility for bladder disease", *Journal of Urology* **167** (2002), 1492–1496.
[58] S.A. McLaughlin et al., "Influence of frozen-section analysis of sentinel lymph node and lumpectomy margin status on reoperation rates in patients undergoing breast-conservation therapy", *Journal of the American College of Surgeons* **206** (2008), 76–82.
[59] F.T. Nguyen et al., "Intraoperative evaluation of breast tumor margins with optical coherence tomography", *Cancer Research* **69** (2009), 8790–8796.
[60] W. Luo et al., "Optical biopsy of lymph node morphology using optical coherence tomography", *Technology in Cancer Research & Treatment* **4** (2005), 539–547.
[61] F.T. Nguyen et al., "Optical coherence tomography: The intraoperative assessment of lymph nodes in breast cancer", *IEEE Engineering in Medicine and Biology Magazine* **29** (2010), 63–70.
[62] A. Ahmad et al., "Cross-correlation-based image acquisition technique for manually-scanned optical coherence tomography", *Optics Express* **17** (2009), 8125–8136.
[63] A.M. Zysk and S.A. Boppart, "Computational methods for analysis of human breast tumor tissue in optical coherence tomography images", *Journal of Biomedical Optics* **11**(1-7), (2006), 054015.
[64] A. Ahmad et al., "Sonification of optical coherence tomography data and images", *Optics Express* **18** (2010), 9934–9944.
[65] K. Zhang and J.U. Kang, "Graphics processing unit accelerated non-uniform fast Fourier transform for ultrahigh-speed,

real-time Fourier-domain OCT", *Optics Express* **18** (2010), 23472–23487.

[66] S.A. Boppart et al., "Optical probes and techniques for molecular contrast enhancement in coherence imaging", *Journal of Biomedical Optics* **10** (1-14), (2005), 041208.

[67] A.L. Oldenburg et al., "Magnetomotive contrast for *in vivo* optical coherence tomography", *Optics Express* **13** (2005), 6597–6614.

[68] A.L. Oldenburg et al., "Phase-resolved magnetomotive OCT for imaging nanomolar concentrations of magnetic nanoparticles in tissues", *Optics Express* **16** (2008), 11525–11539.

[69] R. John et al., "*In vivo* magnetomotive optical molecular imaging using targeted magnetic nanoprobes", *Proceedings of the National Academy of Sciences* **107** (2010), 8085–8090.

[70] X. Liang et al., "Dynamic spectral-domain optical coherence elastography for tissue characterization", *Optics Express* **18** (2010), 14183–14190.

[71] Z. Chen et al., "Optical Doppler tomography", *IEEE Journal of Selected Topics in Quantum Electronics* **5** (2002), 1134–1142.

[72] J.F. de Boer and T.E. Milner, "Review of polarization sensitive optical coherence tomography and Stokes vector determination", *Journal of Biomedical Optics* **7** (2002), 359–371.

[73] C. Xu et al., "Spectroscopic spectral-domain optical coherence microscopy", *Optics Letters* **18** (2006), 1079–1081.

[74] Y. Jiang et al., "Second-harmonic optical coherence tomography", *Optics Letters* **15** (2004), 1090–1092.

[75] D.L. Marks and S.A. Boppart, "Nonlinear interferometric vibrational imaging", *Physical Review Letters* **92** (1-4), (2004), 123905.

[76] P.D. Chowdary et al., "Molecular histopathology by nonlinear interferometric vibrational imaging", *Cancer Research* **70** (2010), 9562–9569.